The influence of defects on the effective Young's modulus of a defective solid*

Shen Wei(沈 伟)[a)†], Fan Qun-Bo(范群波)[b)], Wang Fu-Chi(王富耻)[b)], and Ma Zhuang(马 壮)[b)]

[a)] *Central Iron and Steel Research Institute, Beijing* 100081, *China*

[b)] *School of Materials Science and Engineering, Beijing Institute of Technology, Beijing* 100081, *China*

(Received 6 July 2012; revised manuscript received 27 August 2012)

It is difficult to establish structure-property relationships in a defective solid because of its inhomogeneous-geometry microstructure caused by defects. In the present research, the effects of pores and cracks on the Young's modulus of a defective solid are studied. Based on the law of the conservation of energy, mathematical formulations are proposed to indicate how the shape, size, and distribution of defects affect the effective Young's modulus. In this approach, detailed equations are illustrated to represent the shape and size of defects on the effective Young's modulus. Different from the results obtained from the traditional empirical analyses, mixture law or statistical method, for the first time, our results from the finite element method (FEM) and strict analytical calculation show that the influence of pore radius and crack length on the effective Young's modulus can be quantified. It is found that the longest crack in a typical microstructure of ceramic coating dominates the contribution of the effective Young's modulus in the vertical direction of the crack.

Keywords: defects, effective Young's modulus, conservation of energy, pore radius and crack length

PACS: 46.05.+b, 62.20.de **DOI:** 10.1088/1674-1056/22/4/044601

1. Introduction

The determining of effective elastic properties of inhomogeneous materials has applications in different fields such as materials science, structural mechanics, and geophysics.[1] It has been shown that mechanical properties are strongly dependent on all kinds of defects in material.[2,3] The defective microstructure greatly influences the effective elastic modulus and further influences the material behaviors. Depending on the shape, size, and the distribution of the defects, the overall properties of many engineering and geological materials will possess anisotropies to different degrees. Usually, microscopically defective material can be equivalently replaced by a macroscopically homogeneous continuum medium with properly defined effective properties.[4] However, effective properties are related to the detailed microstructures of inhomogeneities.

The elastic modulus of defective solids has been studied both experimentally and theoretically. Ramakrishnan and Arunachalam[5] proposed the equations for effective elastic moduli of porous solids using the principle of statistical continuum mechanics. In Ref. [6], some independent elastic constants were derived by the Mori–Tanaka's mean-field theory in conjunction with Eshelby's solution. Theoretical approaches such as molecular dynamic simulations, finite element analysis, and classical elastic shell theory were frequently used to estimate the elastic properties of different materials.[7–10] Feng and Yu[11] developed a method of estimating the effects of microdefect interaction on the effective elastic properties of heterogeneous solids. Also, in Refs. [12]– [14], the authors used the object-oriented finite element (OOF) method[15] to study the effective Young's modulus of coating with actual microstructure, and most of their studies only referred to the relationship between porosity and the effective Young's modulus. However, no detailed mathematical formulation has been developed to explain how the shape, size, and distribution of defects, including pores and cracks, affect the effective elastic modulus.

In this paper, novel mathematical formulations are proposed to indicate the relationship between defects and the effective Young's modulus by the law of the conservation of energy. In the mathematical expression, the effect of the defects on the effective Young's modulus is an independent variable only affected by the defects themselves. If the defect is far from the plate boundaries, it is found that there is no relationship between the defect location in the solid and the effective Young's modulus; for the first time, the effective Young's modulus affected by the radius of the pore and the length of the crack is expressed mathematically in detail. Using the newly developed mathematical expression, we further analyze the contribution of the longest crack in a typical microstructure of ceramic coating to the effective Young's modulus in vertical direction of the crack.

2. Mathematical formulation of the effective Young's modulus affected by defects

When loads are gradually applied to a solid body, they will lead to deformation of the material. Provided that no en-

*Project supported by the National Natural Science Foundation of China (Grant No. 50801005).

†Corresponding author. E-mail: wells.shen@gmail.com

© 2013 Chinese Physical Society and IOP Publishing Ltd

ergy is lost in the form of heat, then the external work done by the loads will be converted into internal work called strain energy.

A rectangular plate of unit thickness shown in Fig. 1(a) is subjected to the uniform normal stress σ on the top, and its bottom is fixed. If the stress σ is gradually increased from 0 to σ_0, the force f is gradually increased from 0 to $\sigma_0 l$ correspondingly; when the final displacement of the top of the plate reaches Δh, the external work becomes

$$W = \int_0^{\Delta h} f \,\mathrm{d}h = \frac{\sigma_0 \cdot l \cdot \Delta h}{2}, \tag{1}$$

where h is the height of the plate, l is width of the plate, Δh is the displacement.

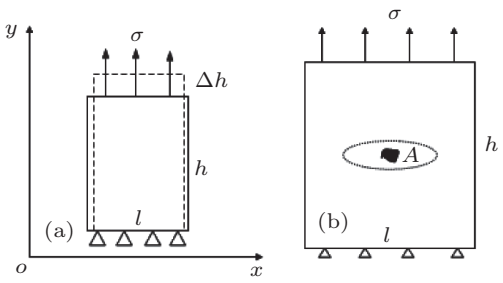


Fig. 1. (a) Plate without defect inside and (b) plate with defect inside each subjected to a uniform normal stress.

If the material behaves in an isotropic elastic manner, for a plate without defects inside, by Hooke's law we obtain the strain energy as

$$U = \int_0^{\varepsilon} \sigma_0 \,\mathrm{d}\varepsilon \int \mathrm{d}x \int \mathrm{d}y = \frac{1}{2} E \varepsilon^2 \int_S \mathrm{d}S = \frac{1}{2} \frac{\sigma_0^2}{E_0} \int_S \mathrm{d}S, \tag{2}$$

where E_0 is the Young's modulus of the non-defective bulk material, ε is the normal strain. Based on the principle of conservation of energy, $W = U$, the Δh can be expressed as

$$\Delta h = \frac{1}{2} \frac{\sigma_0^2}{E_0} \cdot l \cdot h \cdot \frac{2}{\sigma_0 \cdot l} = \frac{\sigma_0 \cdot h}{E_0}. \tag{3}$$

In plane stress, the effective Young's modulus is found to be

$$E_{\mathrm{eff}} = \frac{\sigma_0}{\varepsilon_0} = \frac{\sigma_0}{\Delta h / h} = E_0. \tag{4}$$

With defects inside the plate shown in Fig. 1(b), Saint–Venant's principle claims that the localized effects caused by any inside defect acting on the body will dissipate or smooth out within regions that are sufficiently far from the location of defects. Furthermore, the resulting stress distribution in these regions will be the same as that caused by any other statically equivalent load applied to the body without defects inside. Because of the localized effects caused by the defect, a nonlinear stress region will occur around the defect, section A. Then, the total strain energy is rewritten as

$$U = \frac{1}{2} \frac{\sigma_0^2}{E_0} [(1-\rho) \cdot hl - A] + \int_A \omega \,\mathrm{d}A, \tag{5}$$

where the porosity is ρ; ω is strain energy density at section A, and $\int_A \omega \,\mathrm{d}A$ is the strain energy of section A.

Accordingly, $W = U$ can be further expressed as

$$\frac{\sigma_0 \cdot l \cdot \Delta h}{2} = \frac{1}{2} \frac{\sigma_0^2}{E_0} [(1-\rho) \cdot hl - A] + \int_A \omega \,\mathrm{d}A, \tag{6a}$$

$$\Delta h = \frac{(\sigma_0^2 / E_0)[(1-\rho) \cdot hl - A] + 2 \int_A \omega \,\mathrm{d}A}{\sigma_0 \cdot l}. \tag{6b}$$

The effective in-plane elastic modulus E_{eff} can be predicted by

$$\frac{1}{E_{\mathrm{eff}}} = \frac{1}{E_0} \left(1 - \rho - \frac{A}{hl}\right) + \frac{2 \int_A \omega \,\mathrm{d}A}{\sigma_0^2 \cdot hl}, \tag{7}$$

where $\int_A \omega \,\mathrm{d}A$ can be calculated from strain energy equation as follows:

$$\int_A \omega \,\mathrm{d}A = \frac{1}{2E_0} \int_A [(\sigma_x^2 + \sigma_y^2) - 2\nu \sigma_x \sigma_y + 2(1+\nu)\tau_{xy}^2] \,\mathrm{d}A. \tag{8}$$

Here, A is also a function related to defects in shape and size: one defect with a certain shape and size determines one value of A; σ_x, σ_y, and τ_{xy} are Cartesian coordinate stress distribution inside A, which is related to external stress σ_0. Because E_{eff} in Eq. (8) is not affected by external stress σ_0, $2 \int_A \omega \,\mathrm{d}A / \sigma_0^2$ can be simplified into

$$\frac{2 \int_A \omega \,\mathrm{d}A}{\sigma_0^2} = \frac{f(A)}{E_0}, \tag{9}$$

where

$$f(A) = \int_A \left[\frac{(\sigma_x^2 + \sigma_y^2) - 2\sigma_x \sigma_y + 2(1+\nu)\tau_{xy}^2}{\sigma_0^2} \right] \mathrm{d}A. \tag{10}$$

Thus,

$$\frac{1}{E_{\mathrm{eff}}} = \frac{1}{E_0} (1 - \rho - \frac{A}{hl}) + \frac{f(A)}{E_0 \cdot hl}, \tag{11a}$$

$$E_{\mathrm{eff}} = E_0 \cdot \frac{hl}{(1-\rho) \cdot hl + [f(A) - A]}. \tag{11b}$$

Here, $[f(A) - A]$ is only related to the shape and size of defect, which can be defined briefly as

$$C_{\mathrm{E}} = f(A) - A. \tag{12}$$

Then E_{eff} is given by

$$E_{\mathrm{eff}} = E_0 \cdot \frac{hl}{(1-\rho) \cdot hl + C_{\mathrm{E}}}. \tag{13}$$

Equation (13) is the effect of defect on the Young's modulus of a defective solid, which indicates that if a defect is far from the boundaries of a solid, there is no relationship between the defect location in the model and the effective Young's modulus.

If there are n defects and defects are not affected by each other, the effective Young's modulus can be expressed as follows:

$$E_{\mathrm{eff}} = E_0 \cdot \frac{hl}{(1-\rho) \cdot hl + \sum_{i=1}^{n} C_{\mathrm{E}}(i)}. \tag{14}$$

2.1. Effects of pores on the effective elastic modulus

A rectangular plate of unit thickness with a circular pore of radius a shown in Fig. 2 is loaded on the top by the traction distribution σ which is gradually increased from 0 to σ_0, while the bottom is fixed. Provided that the material behaves in a linear-elastic manner, the stress distribution acting on section A can be determined from mathematical analysis as follows:

$$\begin{aligned}
\sigma_x &= \frac{1}{2}\sigma\left[2+\left(\frac{3a^4}{r^4}-\frac{2a^2}{r^2}\right)\cos 4\theta-\frac{3a^2}{r^2}\cos 2\theta\right],\\
\sigma_y &= \frac{1}{2}\sigma\left[-\left(\frac{3a^4}{r^4}-\frac{2a^2}{r^2}\right)\cos 4\theta-\frac{a^2}{r^2}\cos 2\theta\right],\\
\tau_{xy} &= \frac{1}{2}\sigma\left[\left(\frac{3a^4}{r^4}-\frac{2a^2}{r^2}\right)\sin 4\theta-\frac{a^2}{r^2}\sin 2\theta\right].
\end{aligned} \tag{15}$$

So $\int_A \omega \mathrm{d}A/\sigma_0^2$ is then given from Eqs. (9) and (15) as

$$\frac{\int_A \omega \mathrm{d}A}{\sigma_0^2} = \frac{1}{2E_0}\int_A f\left(\frac{a}{r},\theta\right)\mathrm{d}A, \tag{16}$$

where

$$\begin{aligned}
f\left(\frac{a}{r},\theta\right) &= \frac{1}{4}\left[2+\left(\frac{3a^4}{r^4}-\frac{2a^2}{r^2}\right)\cos 4\theta-\frac{3a^2}{r^2}\cos 2\theta\right]^2\\
&\quad+\frac{1}{4}\left[-\left(\frac{3a^4}{r^4}-\frac{2a^2}{r^2}\right)\cos 4\theta-\frac{a^2}{r^2}\cos 2\theta\right]^2\\
&\quad-\frac{v}{2}\left[2+\left(\frac{3a^4}{r^4}-\frac{2a^2}{r^2}\right)\cos 4\theta-\frac{3a^2}{r^2}\cos 2\theta\right]\\
&\quad\times\left[-\left(\frac{3a^4}{r^4}-\frac{2a^2}{r^2}\right)\cos 4\theta-\frac{a^2}{r^2}\cos 2\theta\right]\\
&\quad+\frac{(1+v)}{2}\left[\left(\frac{3a^4}{r^4}-\frac{2a^2}{r^2}\right)\sin 4\theta\right.\\
&\quad\left.-\frac{a^2}{r^2}\sin 2\theta\right]^2.
\end{aligned} \tag{17}$$

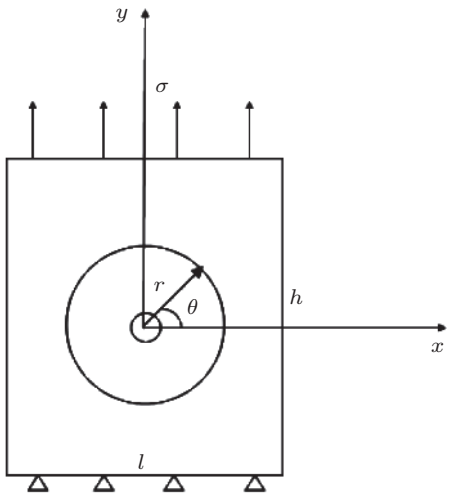


Fig. 2. Stretched plate with a small pore inside.

Thus, C_E in Eq. (13) can be written briefly as

$$C_\mathrm{E} = \int_{A(a)} f\left(\frac{a}{r},\theta\right)\mathrm{d}A - A(a). \tag{18}$$

Although C_E values can be obtained by integral equation of $A(a)$, $A(a)$ is not clear. In our research, C_E values with different values of pore radius a are calculated from FEM analyses, and the results are plotted in Fig. 3. From Fig. 3, C_E can be mathematically fitted to

$$C_\mathrm{E} = \alpha_\mathrm{p}\cdot a^2, \quad \alpha_\mathrm{p} \approx 9.57. \tag{19}$$

Combining Eq. (13) and Eq. (19) yields

$$E_\mathrm{eff} = E_0\cdot\frac{hl}{(1-\rho)\cdot hl+\alpha_\mathrm{p}\cdot a^2}. \tag{20}$$

If defects are composed of n pores and pores are not affected by each other, the effective elastic modulus can be expressed as follows:

$$E_\mathrm{eff} = E_0\cdot\frac{hl}{(1-\rho)\cdot hl+\alpha_\mathrm{p}\sum_{i=1}^{n}a_i^2}. \tag{21}$$

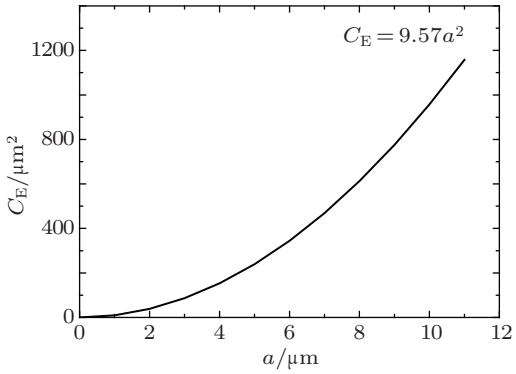


Fig. 3. Variation of C_E with pore radius, obtained from FEM analysis.

2.2. Effects of cracks on effective elastic moduls

A rectangular plate of unit thickness with a crack of length $2a$ is shown in Fig. 4(a), and the stress distribution acting on section A can be defined from a mathematical analysis:

$$\begin{aligned}
\sigma_x &= \sigma\sqrt{\frac{a}{2r}}\cos\frac{\theta}{2}\cdot\left(1-\sin\frac{\theta}{2}\cdot\sin\frac{3\theta}{2}\right),\\
\sigma_y &= \sigma\sqrt{\frac{a}{2r}}\cos\frac{\theta}{2}\cdot\left(1+\sin\frac{\theta}{2}\cdot\sin\frac{3\theta}{2}\right),\\
\tau_{xy} &= \sigma\sqrt{\frac{a}{2r}}\cos\frac{\theta}{2}\cdot\sin\frac{\theta}{2}\cdot\cos\frac{3\theta}{2}.
\end{aligned} \tag{22}$$

$\int_A \omega \mathrm{d}A/\sigma_0^2$ is then given from Eq. (9) and Eq. (22) as follows:

$$\frac{\int_A \omega \mathrm{d}A}{\sigma_0^2} = \frac{1}{2E_0}\int_A f\left(\frac{a}{r},\theta\right)\mathrm{d}A, \tag{23}$$

where

$$f\left(\frac{a}{r},\theta\right) = \frac{a}{r}\left\{\left(\left[\cos\frac{\theta}{2}\cdot\left(1-\sin\frac{\theta}{2}\cdot\sin\frac{3\theta}{2}\right)\right]^2\right.\right.$$

$$+\left[\cos\frac{\theta}{2}\cdot\left(1+\sin\frac{\theta}{2}\cdot\sin\frac{3\theta}{2}\right)\right]^2$$
$$-2v\left[\cos\frac{\theta}{2}\cdot\left(1-\sin\frac{\theta}{2}\cdot\sin\frac{3\theta}{2}\right)\right]$$
$$\times\left[\cos\frac{\theta}{2}\cdot\left(1+\sin\frac{\theta}{2}\cdot\sin\frac{3\theta}{2}\right)\right]$$
$$+2(1+v)\left[\cos\frac{\theta}{2}\cdot\sin\frac{\theta}{2}\cdot\cos\frac{3\theta}{2}\right]^2\Bigg\}. \quad (24)$$

Thus, C_{E} in Eq. (13) can be written briefly as

$$C_{\mathrm{E}}=\int_{A(a)} f\left(\frac{a}{r},\theta\right)\mathrm{d}A-A(a). \quad (25)$$

Since the porosity induced by a crack is so small that the porosity ρ can be assumed to be zero, E_{eff} can be simply given from Eq. (13) as

$$E_{\mathrm{eff}}=E_0\cdot\frac{hl}{hl+C_{\mathrm{E}}}, \quad (26)$$

where C_{E} values with different transverse crack length $2a$ calculated from FEM analyzes are plotted in Fig. 5. From Fig. 5, C_{E} can be mathematically fitted to

$$C_{\mathrm{E}}=\alpha_{\mathrm{c}}\cdot a^2, \quad \alpha_{\mathrm{c}}\approx 6.26. \quad (27)$$

As shown in Eqs. (19) and (27), α_{c} is less than α_{p}. However, the crack length is always much larger than pore diameter in an actual solid, which might induce a much stronger influence than pores.

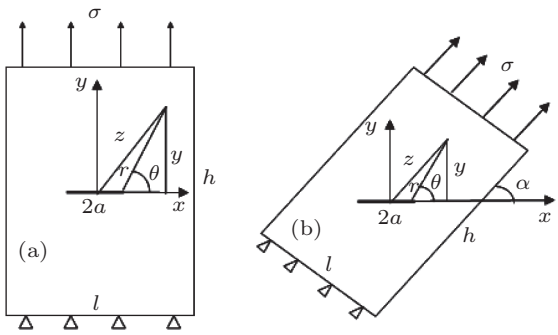


Fig. 4. An isotropic plate with a straight crack (a) and an isotropic plate with an inclined crack (b) inside, each subjected to a uniform normal stress.

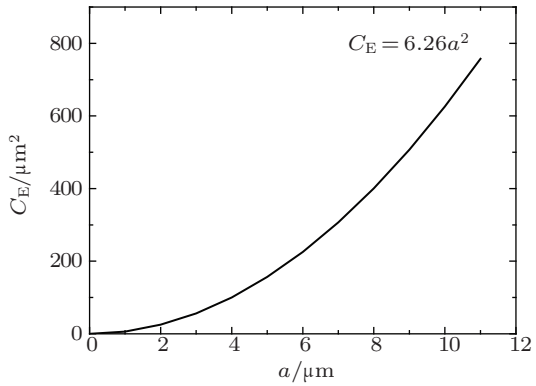


Fig. 5. Variation of C_{E} with crack length, obtained from FEM analysis.

Combining Eq. (26) and Eq. (27) yields

$$E_{\mathrm{eff}}=E_0\cdot\frac{hl}{hl+\alpha_{\mathrm{c}}\cdot a^2}. \quad (28)$$

If defects are composed of n cracks and the cracks are not affected by each other, the effects of cracks on effective elastic modulus can be expressed as follows:

$$E_{\mathrm{eff}}=E_0\cdot\frac{hl}{hl+\sum_{i=1}^{n}C_{\mathrm{E}}(i)}, \quad (29a)$$

$$E_{\mathrm{eff}}=E_0\cdot\frac{hl}{hl+\alpha_{\mathrm{c}}\sum_{i=1}^{n}a_i^2}. \quad (29b)$$

Consider that a crack in an infinite plate, normal to the crack plane, is oriented at an angle α with respect to the stress axis as shown in Fig. 4(b), thus, we obtain

$$E_{\mathrm{eff}}=E_0\cdot\frac{hl}{hl+C_{\mathrm{E}}}, \quad (30)$$

where

$$C_{\mathrm{E}}=\int_{A(a,\alpha)} f\left(\frac{a}{r},\theta,\alpha\right)\mathrm{d}A-A(a,\alpha). \quad (31)$$

3. Calculation results of ceramic coating

A typical microstructure of ceramic coating from the cross-section view by scanning electron microscopy (SEM) is shown in Fig. 6. It includes yttria partially stabilized zirconia (YSZ) and defects. In our previous research,[16] Fig. 6 has also been used to indicate the relationship between defect and the effective thermal conductivity. The model size is 120 μm×90 μm with a total porosity of 3.68%.

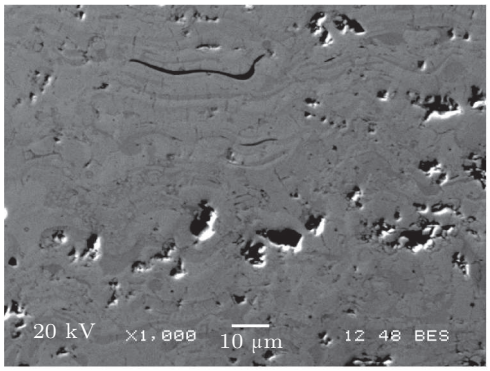


Fig. 6. Cross-sectional microstructure of ceramic coating (120 μm×90 μm).

With one pixel corresponding to one finite element, the collection of pixels can be changed into a collection of finite elements. In this way, a finite element grid model with 4.32×10^4 quadrilateral elements in Fig. 7 based on the actual

microstructure of ceramic coating is generated by digital image processing theory and the finite element mesh generation principle.[17] In addition, the results of the effective Young's modulus are obtained through static uniaxial loading calculations. The model is loaded on the top by the maximum traction distribution σ_0, while the bottom is fixed. With the FEM, the displacement Δh is calculated. Additionally, the Young's modulus of the non-defective bulk material of YSZ material is $E_0 = 214$ GPa. By employing Eq. (32), the effective Young's modulus in the y direction is calculated from

$$E_{\text{eff}} = \frac{\sigma_0 \cdot h}{\Delta h} \tag{32}$$

to be $E_{\text{eff}} = 160$ GPa.

Denote the longest transverse crack in Fig. 6 with approximate length 37 μm as No. 1 defect in Eq. (14), then $C_{\text{E}}(1)$ in Eq. (27) can be expressed as

$$C_{\text{E}}(1) = \alpha_{\text{c}} \cdot a^2 \approx 6.26 \times 18.5^2 = 2142\ \mu\text{m}^2. \tag{33}$$

Then, equation (14) can be rewritten as

$$E_{\text{eff}} = E_0 \cdot \frac{hl}{(1-\rho)\cdot hl + C_{\text{E}}(1) + \sum_{i=2}^{n} C_{\text{E}}(i)}, \tag{34a}$$

$$160 = 214 \times \frac{90 \times 120}{(1-0.0368) \times 90 \times 120 + 2142 + \sum_{i=2}^{n} C_{\text{E}}(i)}. \tag{34b}$$

Thus,

$$\sum_{i=2}^{n} C_{\text{E}}(i) = 1900\ \mu\text{m}^2. \tag{35}$$

It is found that $C_{\text{E}}(1) > \sum_{i=2}^{n} C_{\text{E}}(i)$, which indicates that the longest transverse crack plays the most important role for the effective Young's modulus along the vertical direction in all the defects, including all the pores and other cracks in Fig. 6.

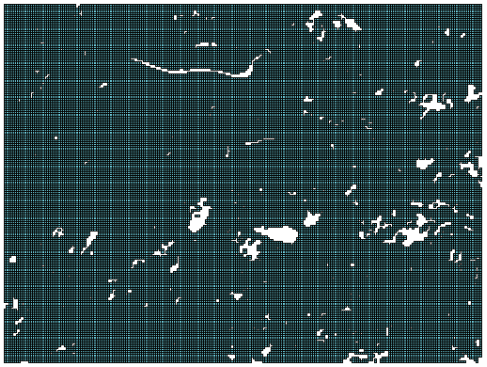


Fig. 7. Finite element grid model of ceramic coating (240×180).

4. Conclusion

Based on the law of the conservation of energy, mathematical formulations of the effective in-plane Young's modulus of defective solids are proposed.

(i) With the aid of strict analytical calculation, the contribution of defects on the effective Young's modulus of defective solids is expressed as a function of an independent variable C_{E}, which is only affected by the defects. It is found that if the defects are far from the boundaries of solid and not affected by each other, there is no relationship between the defect location in the solid and the effective Young's modulus.

(ii) By means of analytical mathematical formulations in conjunction with FEM results, C_{E} of a pore with radius a is fitted to $C_{\text{E}} = \alpha_{\text{p}} \cdot a^2$; C_{E} of a straight crack with length $2a$ is fitted to $C_{\text{E}} = \alpha_{\text{c}} \cdot a^2$. Though α_{c} is less than α_{p}, a long crack induces a much stronger influence than a pore.

(iii) The effective elastic modulus of ceramic coating based on a typical actual microstructure is studied. The results indicate that the longest transverse crack plays the most important role for the effective Young's modulus in the vertical direction of the crack in all the defects combined.

References

[1] Carvalho F C and Labuz J F 1996 *Int. J. Solids Struct.* **33** 4119

[2] Sun Y, Eripret C and Rousselier G 1995 *Eng. Fract. Mech.* **5** 337

[3] Podrezov Y N, Lugovoi N L and Slyunyaev V N 1999 *Powder Metall. Met. Ceram.* **38** 198

[4] Ju J W and Chen T M 1994 *Acta Mech.* **103** 123

[5] Ramakrishnan N and Arunachalam V S 1990 *J. Mater. Sci.* **25** 3930

[6] Zhao Y H, Tandom G P, Weng G J, Brunswich N and Jersey N 1989 *Acta Mech.* **76** 105

[7] Lau K T, Chipara M, Ling H Y, Ling H Y and Hui D 2004 *Compos. B: Eng.* **35** 95

[8] Fan T Y, Xie L Y, Fan L and Wang Q Z 2011 *Chin. Phys. B* **20** 076102

[9] Liu Z H and Shang J X 2012 *Chin. Phys. B* **21** 016202

[10] Liu S S, Wen Y H and Zhu Z Z 2008 *Chin. Phys. B* **17** 2621

[11] Feng X Q and Yu S W 2000 *Theor. Appl. Fract. Mech.* **34** 225

[12] Michlik P and Berndt C 2006 *Surf. Coat. Technol.* **201** 2369

[13] Wang Z, Kulkarni A, Deshpande S, Nakamura T and Herman H 2003 *Acta Mater.* **51** 5319

[14] Jadhav A D, Padture N P, Jordan E H, Gell M, Miranzo P and Fuller J E 2006 *Acta Mater.* **54** 3343

[15] Langer S A, Carter W C and Fuller E R 1997 "Object Oriented Finite Element Analysis for Materials Science", Center for Theoretical and Computational Materials Science and the Information Laboratory at the NIST, 1997, URL: www.ctcms.nist.gov/oof/ (10/2004)

[16] Shen W, Fan Q B, Wang F C and Ma Z 2012 *Appl. Math. Model.* **36** 1995

[17] Shen W, Fang Q B, Wang F C and Ma Z 2009 *Comput. Mater. Sci.* **46** 600